

IMPLICATIONS AND MITIGATION OF RADIATION EFFECTS ON THE CERN SPS OPERATION DURING 2021

Y. Q. Aguiar, G. Lerner, M. Cecchetto, R. García Alía, K. Bilko, A. Zimmaro,
M. Brucoli, S. Danzeca, T. Ladzinski, A. Apollonio, J. B. Potoine
CERN, CH-1211, Geneva, Switzerland

Abstract

During the Long Shutdown 2 (LS2, 2019-2020), the CERN accelerator complex has undergone major upgrades, mainly in preparation for the High-Luminosity (HL) LHC era, the ultimate capacity for its physics production. Therefore, several novel equipment and systems were designed and deployed throughout the accelerator complex. To comply with the radiation level specifications and avoid machine downtime due to radiation effects, the electronics systems exposed to radiation need to follow Radiation Hardness Assurance (RHA) methodologies developed and validated by the Radiation to Electronics (R2E) project at CERN. However, the establishment of such procedures is not yet fully implemented in the LHC injector chain, and some R2E failures were detected in the SPS during the 2021 operation. This work is devoted to describing and analysing the R2E failures and their impact on operation, in the context of the related radiation levels and equipment sensitivity.

INTRODUCTION

Within the CERN accelerator complex, several critical systems are designed to operate under harsh environment composed of a mixed radiation field. However, besides the adoption of different radiation hardened (rad-hard) solutions for electronics, the usage of Commercial Off-the-Shelf (COTS) products is still widely exploited. This is mostly motivated by some limitations of the available rad-hard components that do not meet the specifications required for the accelerator systems, as well as by the cost of the rad-hard electronics, which can be up to a factor 100 more expensive than their COTS counterparts. Therefore, in order to prevent radiation-induced failures and their consequent impact on the accelerator availability, Radiation Hardness Assurance (RHA) methodologies are used not only to mitigate the failures during the operation lifetime, but also for the sake of prevention [1–3].

One example of a safety critical system is the Access or Personnel Protection System (PPS) which not only controls the access to the accelerator, but also interlocks its critical components in case of potential human presence underground [4]. Therefore, as will be shown in this paper, R2E failure events are capable of inducing beam dumps, negatively impacting the availability of the accelerators. In this context, this work presents the implications of the R2E failures observed during the CERN's Super Proton Synchrotron (SPS) operation in 2021 and the consequent mitigation measures taken to improve the availability of the accelerator.

SPS ACCESS SYSTEM AND R2E

The access system provides permanent protection of the personnel implementing several safety-interlock functions. It is based on a three-layer Programmable Logic Controller (PLC) architecture. The sixteen site layer controllers together with sixteen access point controllers constantly monitor some 23'000 I/O channels and make sure that whenever there is ongoing access, no beam can be present in the SPS complex. Therefore, the system has a direct impact on the operation and availability of the SPS accelerator. During the past Long Shutdown (2019 – 2020), the SPS PPS underwent a renovation campaign where the system was fully replaced [4, 5].

The PLC controllers are connected to Elements Important for Safety (EIS) such as personnel and material access devices, doors, extractor kickers, beam absorbers and etc. Given the severity of a failure occurrence and the implementation constraints, the adopted safety PLC system was designed with a Safety Integrity Level of 3. Whenever a failure is observed in the PLCs, the system goes to a fail-safe state to prevent a catastrophic event from happening as, for example, the presence of a person in the tunnel while there is beam injected in the machine. Therefore, the fail-safe state in this case is to dump the injected beam impacting on the availability of the accelerator. During the physics run in 2021, the SPS PPS has experienced an important number of failures on the input/output (I/O) cards that connect the PLC controllers to the EIS devices. Based on the failure signature, the root cause for such events was classified as radiation effects to electronics, namely, Single-Event Upsets (SEUs) in the memories. Figure 1 provides the observed number of R2E induced failures as a function of the integrated SPS injected intensity.

A total of 75 events have been recorded in the I/O cards, and, although not all of them lead to beam dumps, their occurrence can significantly increase the downtime of the machine as the modules need to be manually reset during a beam stop. Thanks to the several mitigation measures timely taken in place, the failure rate was reduced throughout the SPS operation and the annual integrated injected intensity reached $1.17 \cdot 10^{19}$ charges [6]. Table 1 provides an overview of the total number of sensitive cards in each electronics rack location in the SPS tunnel, the total number of R2E induced failures, the High-Energy Hadron equivalent (HEHeq) and thermal neutron (ThN) particle fluences measured by Bat-Mon monitors [7, 8] and the respective R factor which is the ratio between the ThN and HEHeq particle fluences.

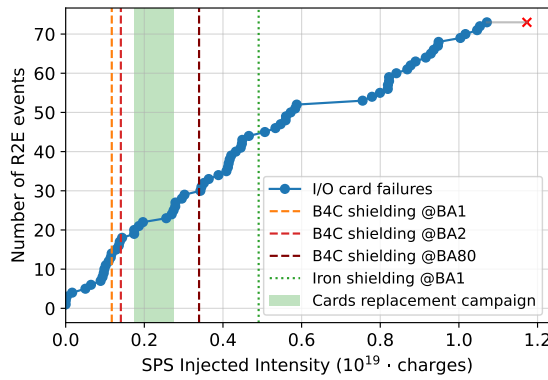


Figure 1: Number of R2E-induced I/O card failures as a function of the integrated injected intensity.

Given the higher failure rates at BA1, BA2 and BA80, the mitigation actions were focused mainly on those locations.

R2E MITIGATION MEASURES

As shown in Fig. 1, as soon as the first events were identified as possible R2E induced failures, the most practical intervention, considering its rapid installation and efficiency against thermal neutrons, was the deployment of boron carbide (B4C) shielding in front of the sensitive components in the electronics racks. The B4C layers can be found as rigid tiles (99% B4C) or flexible layers (80% B4C) which can be easily cut with a scissor and adapted to the installation requirements. In Fig. 2, the neutron spectra in a mixed radiation field facility (CHARM) [9, 10] is simulated using the FLUKA Monte Carlo code [11–13], showing the efficiency of the B4C shielding in the absorption of low-energy neutrons ($E < 1 \text{ eV}$). Despite the effectiveness of B4C in absorbing the thermal neutrons, little impact was observed in the failure rate. As confirmed by BatMon measurements, it was not possible to cover the 4π solid angle of the equipment racks to effectively reduce the neutron fluence impinging the sensitive component. Another mitigation approach concerned the replacement of the I/O cards as the vendor confirmed the batch of electronics provided to CERN

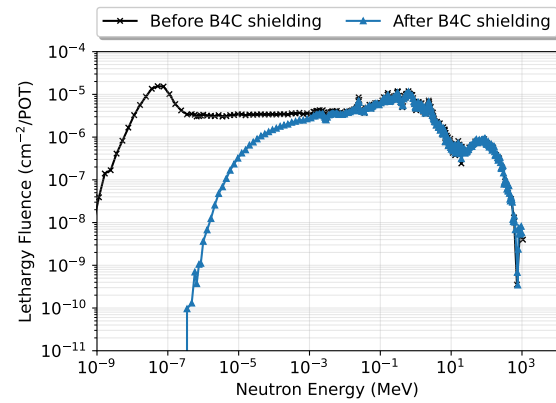


Figure 2: FLUKA simulation of the neutron spectra in MO position in the CHARM facility [9, 10] and the absorption efficiency of a boron carbide (B4C) shielding.

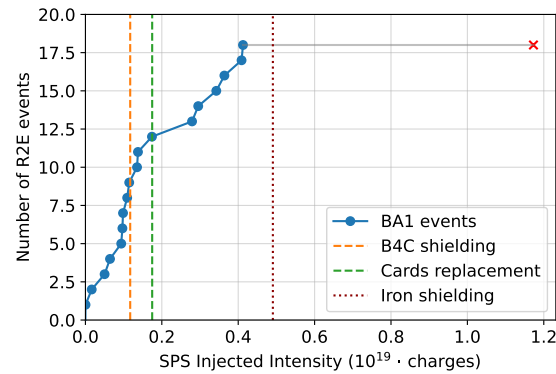


Figure 3: Number of R2E events at BA1 location as a function of the integrated SPS injected intensity and mitigation actions. Red cross marks the end of SPS operation.

was not ULA (Ultra-Low Alpha) compliant. Therefore, the components showed a higher contaminant decay from the package material, leading to a higher sensitivity to secondary alpha particles. As shown in Fig. 1, a replacement campaign was carried out to replace all the non-ULA compliant cards. The impact of these two actions can be seen in the failure rate in the BA1 electronics rack shown in Fig. 3.

Table 1: Number of Sensitive Electronics, Number of R2E Induced Failures and Particle Fluence for Each Rack Location in the SPS during Physics Run in 2021

| Rack location | Total number of | | Particle fluence ($10^8 \cdot \text{cm}^{-2}$) | | R factor |
|---------------|-----------------|--------------|--|------|----------|
| | Sensitive cards | R2E failures | HEHeq | ThN | |
| BA1 | 10 | 18 | 1.12 | 1.64 | 1.46 |
| BA2 | 12 | 11 | 0.76 | 2.72 | 3.58 |
| BA3 | 9 | 2 | 0.14 | 0.33 | 2.36 |
| BA80 | 12 | 22 | 0.45 | 3.00 | 6.64 |
| TAG41 | 30 | 6 | 0.15 | 0.05 | 0.34 |
| TCC8 | 9 | 13 | 1.16 | 5.43 | 4.69 |

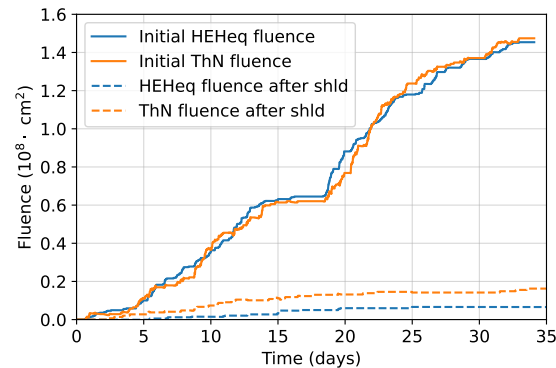


Figure 4: Particle fluences in BA1 measured by BatMons [8] before and after the installation of the iron shielding.

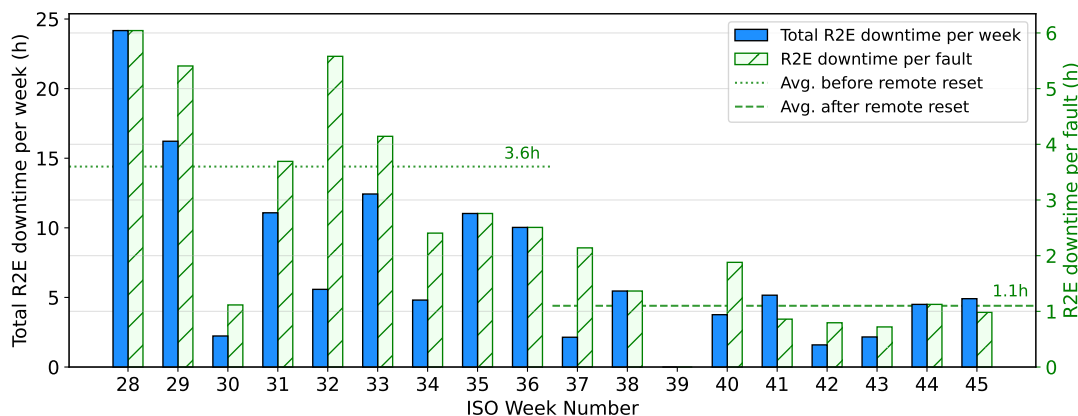


Figure 5: Total R2E downtime per week and average R2E downtime per fault during the SPS operation in 2021.

One can clearly see a change in the slope of the failure rate after the installation of the B4C shielding and the cards replacement. However, as the R2E events at BA1 were still dominating the number of failures in the system, a heavy shielding was proposed as additional mitigation measure. With the installation of a 40-cm iron shielding covering completely the electronics rack, no event was observed until the end of the SPS operation. The particle fluence on the rack was measured before and after the iron shielding installation and it is shown in Fig. 4. By extrapolating the HEHeq fluence measurement with the SPS injected intensity, the normalized HEHeq particle fluence is $5.62 \cdot 10^{-11} \text{ cm}^{-2}/\text{charge}$ and $1.19 \cdot 10^{-12} \text{ cm}^{-2}/\text{charge}$, before and after the shielding installation, respectively. Therefore, a reduction of a factor about 47 was observed for HEHeq fluence while only a reduction factor of about 18 is observed for ThN fluence ($5.54 \cdot 10^{-11} \text{ cm}^{-2}/\text{charge}$ and $3.06 \cdot 10^{-12} \text{ cm}^{-2}/\text{charge}$, before and after the shielding installation, respectively). The lower efficiency in this case can be explained by the neutron scattering around the shielding and the thermalisation process of high energetic neutrons. Due to infrastructure limitations among several others, heavy shielding is not an option for all locations. For instance, together with the BA1 rack, the electronics located in BA80 have shown a high contribution to the system failure rate. However, as the system is located on a metallic structure which cannot support the 17 T of heavy shielding, the relocation of such equipment was proposed. After the end of the SPS operation in 2021, 10 electronics racks have been relocated from the intermediate level, next to the tunnel, to surface locations where the radiation levels are negligible.

As aforementioned, the availability of the access system has a direct impact on the availability of the SPS because a system failure potentially leads to beam dumps. For instance, the 2021 SPS availability reached 73.4%, i.e. an unavailability of 26.6% (806h of downtime). From all the root cause downtime systems, the SPS access system contributed to 16% (131h) of the total downtime, where 127h (97%) corresponded to R2E related faults. However, the SPS access

system reached an availability of 95.4% during 2021, therefore, the system unavailability of 4.6% directly contributed to 4.3% of SPS unavailability in 2021. In this context, besides reducing the failure rate, it is imperative to reduce the downtime of the system by improving the recovery time. In Fig. 5, the total R2E downtime per week and the average R2E downtime per fault is shown for the SPS operation in 2021. In order to improve the recovery time, the system was adapted to provide a remote reset of the faulty modules. In this context, the fault recovery time was reduced due to the suppression of the radiological cool-down time previously required for the manual reset of modules, e.g. from 4 hours cool-down time in BA80 to tens of minutes of intervention. As shown in Fig. 5, besides the reduction of the total R2E downtime per week greatly impacted by the reduction in the failure rate, the average R2E downtime per fault was also reduced from 3.6h to 1.1h after the remote reset approach (about 70% reduction).

CONCLUSIONS

During the SPS operation in 2021, a large number of R2E-related events was observed in the access system. This work presents an overview of the analysis and the several mitigation measures considered in order to improve the reliability of the system. The mitigation approaches spanned from the cards replacement of non-ULA (Ultra Low Alpha) compliant components to the installation of light (Boron Carbide layer) and heavy (Iron wall) shieldings in the electronics racks. Additionally, in order to reduce the average downtime of the system, a remote reset methodology was adopted to avoid the machine access and the cool time requirements for each intervention. Lastly, radiation levels were monitored and ten electronics racks were relocated from the underground rack locations, next to the SPS ring, to safe surface locations. The implications of the R2E failures are also discussed, as it directly impacts the availability of the accelerator, highlighting the importance of avoiding the installation of commercial modules for critical accelerator systems in radiation areas.

REFERENCES

- [1] Y. Q. Aguiar *et al.*, “Radiation to electronics impact on CERN LHC operation: Run 2 overview and HL-LHC outlook,” in *Proc. IPAC’21*, Geneva, Switzerland, 2021, paper MOPAB013, pp. 80–83.
doi:10.18429/JACoW-IPAC2021-MOPAB013
- [2] R. G. Alía *et al.*, “LHC and HL-LHC: Present and future radiation environment in the high-luminosity collision points and rha implications,” *IEEE Trans. on Nucl. Sci. (TNS)*, vol. 65, no. 1, pp. 448–456, 2017.
doi:10.1109/TNS.2017.2776107
- [3] A. Coronetti *et al.*, “Radiation hardness assurance through system-level testing: Risk acceptance, facility requirements, test methodology, and data exploitation,” *IEEE Trans. on Nucl. Sci. (TNS)*, vol. 68, no. 5, pp. 958–969, 2021.
doi:10.1109/TNS.2021.3061197
- [4] T. Ladzinski *et al.*, “Renovation of the SPS personnel protection system: a configurable approach,” in *Proc. 17th Int. Conf. on Accel. and Large Exp. Physics Control Systems (ICALEPCS’19)*, 2020, pp. 395–399.
doi:10.18429/JACoW-ICALEPCS2019-MOPHA078
- [5] T. Ladzinski *et al.*, “SPS personnel protection system: from design to commissioning,” in *Proc. IPAC’21*, Campinas, Brazil, May 2021, pp. 2224–2227.
doi:10.18429/JACoW-IPAC2021-TUPAB314
- [6] K. Bilko *et al.*, “Automated analysis of the prompt radiation levels in the CERN accelerator complex,” presented at IPAC’22, Bangkok, Thailand, Jun. 2022, paper MOPOMS043, this conference.
- [7] S. Danzeca *et al.*, “Wireless IoT in Particle Accelerators: A practical approach with the IoT radiation monitor at CERN,” presented at IPAC’22, Bangkok, Thailand, Jun. 2022, paper TUOXGD2, this conference.
- [8] A. Zimmaro *et al.*, “Testing and validation methodology for a radiation monitoring systems for electronics in particle accelerators,” *IEEE Trans. on Nucl. Sci. (TNS)*, 2022.
10.1109/TNS.2022.3158527
- [9] M. Cecchetto *et al.*, “Impact of thermal and intermediate energy neutrons on sram see rates in the lhc accelerator,” *IEEE Trans. on Nucl. Sci. (TNS)*, vol. 65, no. 8, pp. 1800–1806, 2018. doi:10.1109/TNS.2018.2831786
- [10] J. Mekki *et al.*, “CHARM: A mixed field facility at CERN for radiation tests in ground, atmospheric, space and accelerator representative environments,” *IEEE Trans. on Nucl. Sci. (TNS)*, vol. 63, no. 4, pp. 2106–2114, 2016.
doi:10.1109/TNS.2016.2528289
- [11] C. Ahdida *et al.*, “New capabilities of the FLUKA multi-purpose code,” *Frontiers in Physics*, p. 705, 2022.
- [12] G. Battistoni *et al.*, “Overview of the FLUKA code,” *Annals Nucl. Energy*, vol. 82, pp. 10–18, 2015.
- [13] FLUKA website: <https://fluka.cern>.